Citation: Carlo Solisio, Saleh Al Arni, and Attilio Converti, Adsorption of Inorganic Mercury from Aqueous Solutions onto dry Biomass of Chlorella vulgaris: Kinetic and Isotherm Study, Environmental Technology 2019, vol 40. No. 5, 664-672. https://doi.org/10.1080/09593330.2017.1400114

Adsorption of Inorganic Mercury from Aqueous Solutions onto dry Biomass of *Chlorella vulgaris*: Kinetic and Isotherm Study

Carlo Solisio[a], Saleh Al Arni[b], and Attilio Converti[a]*

[a]*Department of Civil, Chemical and Environmental Engineering, Genoa University, Genoa, Italy*
[b]*Chemical Engineering Department, University of Hai'l, Hai'l, Kingdom of Saudi Arabia*

*Corresponding author.
Attilio Converti, Department of Civil, Chemical and Environmental Engineering, Pole of Chemical Engineering, Genoa University, Via Opera Pia 15, I-16145 Genoa, Italy, Phone: +39-3292104448; Fax: +39-010-3532586; E-mail address: converti@unige.it (A. Converti).

Adsorption of Inorganic Mercury from Aqueous Solutions onto dry Biomass of *Chlorella vulgaris*: Kinetic and Isotherm Study

This study focused on kinetics and equilibrium isotherms of mercury biosorption from water using dry biomass of *Chlorella vulgaris* as biosorbent at pH 5.0. Biosorption tests were performed at 2.0 g/L biomass dosage varying initial Hg concentration from 11.0 to 90.6 mg/L. The Lagergren equation was found to best describe the process, with R^2 of 0.984 and specific rate constant of 0.029±0.004 min^{-1}. Although equilibrium data were well fitted by the Dubinin and Radushkevich isotherm (R^2 = 0.870; q_{DR} = 16.6 mg/g), important insights on phenomenological events occurring at equilibrium were concurrently provided by the Lamgmuir one (R^2 = 0.826; q_0 = 32.6 mg/g; K_L = 0.059 L/mg). FT-IR analysis confirmed that Hg biosorption took place via physisorption. Since *C. vulgaris* is a fresh-water microalga that can be easily cultivated anywhere, these promising results suggest its possible use as an effective, low-cost biosorbent to treat industrial effluents contaminated by this metal.

Keywords: Mercury biosorption; *Chlorella vulgaris*; Kinetics; Equilibrium; FT-IR.

1 Introduction

Industrial heavy metal-containing wastewaters are a significant source of pollution for aquatic resources, because of high toxicity to living organisms including humans; therefore, toxic metal removal is a very urgent problem. In particular, mercury, which is used in pesticides, batteries and paper industry, is one of the priority pollutants listed by the United States Environmental Protection Agency; since it is able to easily cross blood-brain barrier and affect fetal brain, high levels of this metal cause impairment of pulmonary function and kidney, chest pain and dyspnea [1]. Although its presence in aquatic systems has been declining in recent years, there is still a lack of effective, cheap means to treat Hg-containing wastewaters.

At high concentrations, Hg can effectively be removed by conventional methods such as precipitation as hydroxide, membrane filtration or capture onto ionic exchangers. However, these methods are not so efficient when metal concentration is lower than 100 mg/L [2]. For this reason, sorption techniques have been developed; among these, the use of activated carbon would be preferable for its high performance, but it is too expensive for large-scale use. Then, the search for low-cost, easily available adsorbents has promoted the investigation of biomaterials as potential metal sorbents [3]. Particular interest has recently been devoted to microalgae, which, although less effective than superior vegetable beings [4], can more easily and abundantly produced. Among them, the prokaryote *Arthrospira (Spirulina) platensis* and the eukaryote *Chlorella vulgaris* are the most investigated ones, because of their large diffusion worldwide [5,6] and excellent capability of removing heavy metals such as chromium [7] and cadmium [8].

In this work mercury removal by dry biomass of *C. vulgaris* was investigated at different concentrations of this metal, with a view to the mechanisms responsible for its biosorption. Sorption kinetics was studied by means of Lagergren pseudo-first order, Ho and McKay pseudo-second order, intraparticle diffusion, Elovich and simplified Elovich models [9,10]. Isotherm equations of Freundlich, Langmuir, Temkin, Dubinin and Radushkevich, Harkins-Jura, Halsey, Jovanovic and Redlich-Peterson [10,11] were also tested to fit adsorption data at equilibrium. *C. vulgaris* biomass either before or after biosorption was investigated through FT-IR analysis to support the suggestions arose from the isotherm study about possible mechanisms involved in Hg biosorption.

2 Materials and methods

2.1 Chlorella vulgaris *cultivation*

Chlorella vulgaris CCAP211 (Culture Collection of Algae and Protozoa, Argyll, UK) was grown batch-wise in Bold's Basal Medium [12] at 20 ± 1 °C in tubular photobioreactor at photosynthetic photon flux intensity of 82 ± 5 μmol photons m^{-2} s^{-1} under pH control (7.0 ± 0.5) through the daily addition of pure CO_2. Once the stationary phase had been reached after about 20 days of cultivation, cells were centrifuged (model 4226, ALC, Milan, Italy) for 15 min at 3,500 rpm. Recovered cells were washed until pH 7.0, dried at 40°C for 24 h and ground to fine powder, which was sieved through a 120 mesh (0.125 mm) sieve. The undersized fraction was then used as biosorbent.

2.2 Biosorption tests

A 1.0 g/L stock mercury solution (Sigma–Aldrich, Milan, Italy), diluted with distilled water up to the selected concentrations in the range 11.0-90.6 mg/L, was used for biosorption tests, which were carried out in 100-mL Erlenmeyer flasks shaken at 150 rpm at room temperature (20 ± 1°C) using 2.0 g/L of biosorbent. Tests were performed for 2 h, a time sufficient to reach equilibrium. To select the best biosorption conditions, preliminary tests were done either at pH 2.0 or pH 5.0. To this purpose, pH was measured by a pHmeter, model pH 211 (Hanna, Milan, Italy), and controlled at the selected value through the addition of alkaline (0.1 M NaOH) or acidic (0.1 M HNO_3) solutions when necessary. All the other tests were performed at pH 5.0.

Sorption tests were carried out in triplicate, and the results expressed as mean values. Standard deviations between data and mean values never exceeded 6.2%; therefore, no additional statistical analysis was considered to be necessary.

Yield of mercury removal (Y, %) was determined as percentage of sorbate removal:

$$Y(\%) = \left(\frac{C_0 - C}{C_0}\right) \times 100 \quad (1)$$

where C_0 and C are mercury concentrations at the beginning and after a given time.

For FT-IR spectroscopic analysis, biomass as such or plus adsorbed metal recovered at the end of biosorption tests was centrifuged as previously described, dried at 40°C for 24 h and again powdered.

Sorbent biosorption capacity at equilibrium, q_e (mg/g), was calculated as the difference between C_0 and Hg concentration at equilibrium (C_e), both expressed in mg/L, according to the equation:

$$q_e = \frac{V\,(C_0 - C_e)}{M} \quad (2)$$

where V is the solution volume (L) and M the biosorbent mass (g).

2.3 Experimental procedures

Samples of suspensions (2.0 mL) were withdrawn at fixed times and filtered through membrane filters with 0.45 μm-pore diameter (Millipore, Vimodrone, Italy). The filtrate was analyzed for Hg content by an atomic absorption spectrometer, model AA240FS (Varian, Milan, Italy), provided with Vapor Generation Accessory (VGA-77, Varian, Milan, Italy).

Photosynthetic photon flux density was measured in several points over the culture surface using a type sensor quantum/photometer/radiometer, model HD-9021 Delta OHM (Li-Cor Inc., Lincoln, NE, USA).

Samples of biomass either as such or rinsed with deionized water after Hg sorption were prepared for FT-IR analysis by diluting biomass pure powder in KBr disks (1.0%, w/w) and analyzed by a Nicolet 6700 FT-IR instrument (Thermo Fisher, Waltham, MA) equipped with DTGS-KBr detector and OMNIC™ acquisition software. Acquisition was 100 scans for each spectrum, and resolution 2 cm^{-1}.

2.4 Kinetic models

Experimental data of Hg biosorption along the time were analyzed by linearized forms of the five most common adsorption kinetic models, which were already extensively reviewed [9,10]. Kinetic models tested were:

a) pseudo-first order rate equation of Lagergren:

$$\ln(q_e - q) = \ln q_e - k_1 t \quad (3)$$

where q (mg/g) is the adsorbate amount per g of sorbent at time t (min) and k_1 the pseudo-first order rate constant (min^{-1});

b) pseudo-second order model of Ho and McKay:

$$\frac{t}{q} = \frac{1}{k_2 q_e^2} + \frac{1}{q_e} t \quad (4)$$

where k_2 is the second order rate constant (g mg^{-1} min^{-1});

c) intraparticle diffusion model:

$$q = k_{id} t^{0.5} + a \quad (5)$$

where k_{id} (mg g^{-1} $min^{-0.5}$) is the intraparticle diffusion rate constant, while a (mg/g) is proportional to the extent of boundary layer thickness.

d) so-called Elovich model in its integrated form ($q = 0$ at $t = 0$):

$$q = \frac{1}{b}\ln(t + t_0) - \frac{1}{b}\ln t_0 \quad (6)$$

where a (mg g^{-1} min^{-1}) is the initial adsorption rate, b (g/mg) the desorption constant, and $t_0 = 1/ab$;

e) simplified version of Elovich model when $abt >> 1$, i.e. $t_0 \rightarrow 0$:

$$q = \frac{1}{b}\ln(ab) - \frac{1}{b}\ln t. \quad (7)$$

The ability of these models to fit the experimental data was checked comparing the values of determination coefficient (R^2) of their linear regression plots.

2.5 Isotherm models

The most common isotherm models were applied in this study in their linearized forms to investigate isothermal behavior under equilibrium conditions. Comprehensive reviews of them can be found elsewhere [10,11]. The tested isotherm models were:

a) Freundlich model that describes monolayer adsorption with heterogeneous surface:

$$\ln q_e = \ln K_F + \frac{1}{n_F}\ln C_e \quad (8)$$

where K_F is the Freundlich constant ($mg^{1-1/n}$ $L^{1/n}$ g^{-1}) related to sorbent sorption capacity and n_F an empirical parameter (dimensionless) depending on sorption intensity;

b) Langmuir model that supposes monolayer sorption onto a surface with a finite number of identical and homogeneous sites:

$$\frac{1}{q_e} = \frac{1}{q_o} + \frac{1}{q_o K_L}\frac{1}{C_e} \quad (9)$$

where q_0 (mg/g) is the maximum monolayer sorption capacity of sorbent and K_L (L/mg) the Langmuir constant related to both adsorption capacity and energy. Essential characteristics of Langmuir isotherm were also expressed in terms of dimensionless constant separation factor or equilibrium parameter:

$$R_L = \frac{1}{1+K_L C_o}; \quad (10)$$

c) Temkin model [13]:

$$q_e = \frac{RT}{b_T}\ln K_T + \frac{RT}{b_T}\ln C_e, \quad (11)$$

where T is the temperature (K), R the ideal gas constant (8.314 J mol^{-1} K^{-1}), K_T the equilibrium binding constant corresponding to maximum binding energy (L/mg), and b_T (g J mg^{-1} mol^{-1}) the Temkin isotherm constant related to adsorption heat;

d) Dubinin and Radushkevich model based on the Polanyi biosorption potential and Dubinin's minipore filling theory:

$$\ln q_e = \ln q_{DR} - \beta\varepsilon^2 \quad (12)$$

where q_{DR} is the maximum biosorption capacity at equilibrium (mol/g), β the constant of sorption energy (mol^2/J^2), and:

$$\varepsilon = RT\ln\left[1+\frac{1}{C_e}\right] \quad (13)$$

the Polanyi potential (J/mol). From the β value we also estimated the mean sorption energy, E (J/mol), defined as:

$$E = 1/\sqrt{2\beta} \quad (14)$$

that gives information about the nature of biosorption mechanism; if E lies between 8 and 16 kJ/mol the biosorption process can be considered to be controlled by chemical ion-exchange, beyond 16 kJ/mol by a chemical mechanism, while below 8 kJ/mol by a physical one [14];

e) Harkins-Jura adsorption isotherm that accounts for multilayer adsorption and implies existence of heterogeneous pore distribution:

$$\frac{1}{q_e^2} = \frac{B_{\mathrm{HJ}}}{A_{\mathrm{HJ}}} - \frac{1}{A_{\mathrm{HJ}}} \log C_e \,, \quad (15)$$

where B_{HJ} and A_{HJ} are the Harkins-Jura dimensionless constants;

f) Halsey isotherm model that supposes multilayer adsorption and attests the heteroporous nature of adsorbent:

$$\ln q_e = \frac{1}{n_{\mathrm{Ha}}} \ln K_{\mathrm{Ha}} + \frac{1}{n_{\mathrm{Ha}}} \ln C_e \quad (16)$$

where n_{Ha} and K_{Ha} are the Halsey isotherm dimensionless constants;

g) Jovanovic model for monolayer adsorption that takes into account two additional types of molecules collisions as distinct from the Langmuir theory:

$$\ln q_{\mathrm{e}} = \ln q_0 - K_J C_{\mathrm{e}} \quad (17)$$

where K_{J} is a constant (L/mg);

h) Redlich-Peterson isotherm combining Freundlich and Langmuir models, which takes into account the possible heterogeneity of sorbent surface and the presence of adsorption sites with the same adsorption potential:

$$\ln\left(\frac{K_{\mathrm{RP}} C_{\mathrm{e}}}{q_{\mathrm{e}}} - 1\right) = \ln a_{\mathrm{RP}} + \gamma \ln C_{\mathrm{e}} \quad (18)$$

where K_{RP} (L/g), a_{RP} ($\mathrm{L}^{\gamma}/\mathrm{mg}^{\gamma}$) and γ (dimensionless) are adsorption parameters.

The fitness of all isotherm models was checked estimating, in addition to R^2, the root mean square error (RMSE):

$$\mathrm{RMSE} = \sqrt{\frac{1}{N-2} \sum_{i=1}^{N} (q_{\mathrm{e,exp}} - q_{\mathrm{e,cal}})^2} \quad (19)$$

and the chi-square:

$$\chi^2 = \sum_{i=1}^{N} \frac{(q_{\mathrm{e,exp}} - q_{\mathrm{e,cal}})^2}{q_{\mathrm{e,cal}}} \,, \quad (20)$$

where subscripts “exp” and “cal” refer to experimental and calculated values; the lower the values of both statistical parameters, the better the fitting.

3 Results and discussion

3.1 Preliminary tests

As is well known, pH monitoring is crucial for any biosorption system, because it influences the status of both adsorbate and adsorbent, and this is particularly true for biomaterials owing to the presence of outer charges. In particular, mercury adsorption is greatly influenced by its chemical speciation [15]. At pH 2.0 mercury is in fact present in solution exclusively as Hg^{2+}, but increasing pH from 4.0 to 7.0 Hg^{2+} concentration decreases, reaching 100% $Hg(OH)_2$ at pH around 8; thus, in the pH range 2-7, it is present as Hg^{2+} in equilibrium with $Hg(OH)^+$. On the other hand, to select the optimum pH range for metal sorption, it is useful to resort to the biosorbent zero point of charge (pH_{zpc}), i.e. the pH value at which sorbent surface does not carry charges. The pH_{zpc} of *Chlorella vulgaris* biomass used as biosorbent in this study is 4.0 [5]; therefore, equivalence between mercury ionized form and dissociated biomass functional groups was expected in the pH range 5-6.

However, to confirm such an optimum pH range for Hg adsorption, preliminary tests were carried out at two different pH values (2.0 and 5.0) under conditions suggested in previous studies, i.e. biosorbent dosage of 2.0 g/L [5] and Hg concentrations of 23.0-25.0 and 39.2-43.7 mg/L [16,17].

One can see in Table 1 that at both Hg concentration ranges, an increase in pH from 2.0 to 5.0 led to a remarkable raise (37 and 56%, respectively) in equilibrium sorption capacity, hence confirming the validity of selecting pH 5.0 for subsequent kinetic and isothermal studies.

Table 1

3.2 FT-IR study

In order to gain further insight on interactions between Hg ions and *C. vulgaris* biomass, FT-IR analysis was performed on dried biomass either before or after Hg sorption. IR spectrum of pristine *C. vulgaris* biomass (Fig. 1, curve a) shows the main bands typical of lipids and proteins, as summarized in Table 2.

Table 2

IR spectra of biomass after Hg adsorption at pH 5.0 (Fig. 1, curve b) and pH 2.0 (Fig. 1, curve c) showed some differences, with the most significant being the change in shape and relative intensity of the band at 1742 cm^{-1} corresponding to ester groups, which appeared broadened and shifted to about 1720 cm^{-1}.

Figure 1

This difference was relevant in the spectrum of biomass after adsorption at pH 5.0, while was less marked in that recorded at pH 2.0, suggesting an interaction of these functional groups with Hg ions, likely through the oxygen electron lone pairs [5,8]. After adsorption, amide I and II bands were just slightly less intense and broader, thus indicating that protein fraction was only a few influenced by Hg adsorption. After adsorption at pH 5.0, also carboxylate bands (1620 and 1416 cm^{-1}) shifted towards lower frequencies and had their intensity slightly reduced, likely due to a change in coordination of carboxylic group interacting with Hg ions.

These observations are not surprising taking into account that at pH 5.0, i.e. at pH slightly higher than pH_{zpc}, biomass surface retained some additional negative charge belonging to carboxylate. On the other hand, at pH 2.0 biomass had mainly a net positive charge, and free acidic groups were less effective in the coordination or electrostatic interaction with cations than carboxylate. In addition, bands related to carbohydrate fraction (1050 cm^{-1}) had their intensity reduced after Hg adsorption, regardless of pH.

In the high frequency region, the weak band at 3010 cm^{-1} was further weakened by interaction with Hg, suggesting a possible role of unsaturated alkyl chain in the adsorption process, for instance, an interaction with the double bond that represents a region of high electron density. These results as a whole suggest that Hg adsorption onto dry *C. vulgaris* biomass was likely to take place via physisorption rather than chemisorption, mainly through an electrostatic interaction between outer electron-rich functional groups and Hg cations.

3.3 Effect of Hg concentration

Sorption capacity of *C. vulgaris* dry biomass (q) was then investigated at biosorbent concentration of 2.0 g/L varying initial Hg concentration in the range 11.0-90.6 mg/L. Fig. 2A clearly shows that the higher the

initial Hg concentration, the higher the biomaterial sorption capacity, but tests carried out at the two highest Hg concentrations (77.9 and 90.6 mg/L) indicated a worsening of adsorption. One can see in Fig. 2B that more than one half of Hg ions was adsorbed within the first 30-45 min ($Y > 50\%$); thereafter, the ratio of Hg concentration to that at the beginning of runs (C/C_0) gradually declined reaching equilibrium within about 2 h.

Figure 2

Daneshvar et al. [18], who took the same approach to remove dye from water by shrimp shell, reported that such a behavior should be ascribed not only to the increased concentration gradient between bulk and sorbent surface [19], but also to the strengthened interaction between adsorbate and biosorbent [20].

The starting increase of q in all the runs (Fig. 2A) may have been due to physical sorption or ion exchange at biosorbent surface [21], while it reached a constant equilibrium value (q_e) when adsorption stopped, hence suggesting that adsorbed Hg was in a state of dynamic equilibrium with desorbed ions [22]. Biosorption capacity at $C_0 = 48.0$ mg/L was (17.49 mg/g) more than 4-fold that obtained at 11.0 mg/L, which highlights excess of sorbent over Hg, and biosorption consequently depended on biomass structural properties (Fig. 2A). On the other hand, a further increase in C_0 to 77.9 mg/L did not influence biosorption capacity (17.32 mg/g) that suffered even a remarkable decrease (14.56 mg/g) at higher Hg concentration (90.6 mg/L). This behavior suggests the achievement of sorbent saturation conditions at high C_0, and the biosorption process became dependent on the ratio of the initial number of Hg ions to that of available sorption sites. The above maximum Hg sorption capacity agrees with the values reported for other *C. vulgaris* strains (18 mg/g for *C. vulgaris* BCC 15 and 16 mg/g for *C. vulgaris* CCAP211/11B) and compares with those of *Scenedesmus acutus* IFRPD 1020 (20 mg/g) and even of cyanobacteria (27 mg/g for *Tolypothrix tenuis* TISRT 8063 and 19 mg/g for *Calothrix parietina* TISRT 8093) [4]. On the other hand, higher capacities were reported for the green algae *Spirogyra hyalina* (35.7 mg/g) [23] and *Chlamydomonas reinhardtii* (72.2 mg/g) [24], but lower capacities for the red microalga *Porphyridium cruentum* (2.62 mg/g) [25].

3.4 Kinetic study

Kinetics of Hg biosorption onto dry *C. vulgaris* biomass was investigated using the pseudo-first order, pseudo-second order, intraparticle diffusion, Elovich and simplified Elovich models, whose applicability to the system under consideration was assessed mainly on the basis of the assumptions taken in their formulations as well as comparing the coefficient of determination (R^2).

One can see that all the tested linearized models provided satisfactory fitting to the experimental biosorption data ($0.902 \leq R^2 \leq 0.996$), but the pseudo-first order and pseudo-second order models were by far the best ones (Table 3).

Table 3

However, even though the pseudo-second order model gave better fit at different initial Hg concentrations (11.0-90.6 mg/L) (mean $R^2 = 0.996$) than the pseudo-first order one (mean $R^2 = 0.984$), the rate constant showed too high standard deviation with respect to its average value (mean $k_2 = 3.53 \pm 1.33$ g g^{-1} min^{-1}) when compared with the pseudo-first order one (mean $k_1 = 0.029 \pm 0.004$ min^{-1}). Fig. 3 illustrates the pseudo-first order plots of Hg sorption by dry *C. vulgaris* biomass increasing C_0 from 11.0 to 90.6 mg/L. These results point out that Hg biosorption was likely to occur via physisorption rather than a chemisorption mechanism ascribable to cation-exchange capacity of the biosorbent, hence corroborating FT-IR analysis suggestions.

Figure 3

3.5 Isotherm study

The main results of linear fitting by isotherm adsorption models are summarized in Table 4.

Table 4

One can see that the Dubinin-Radushkevich model yielded the best fitting, providing a maximum q_e value at equilibrium (q_{DR} = 16.60 mg/g) close to the experimental one (q_{max} = 17.82 mg/g) as well as the best values of all the statistical criteria (R^2 = 0.870, χ^2 = 3.47, RMSE = 2.76), which means that it explained sufficiently well the relationship between the amount of sorbed Hg and its equilibrium concentration. Although the Freundlich model exhibited the second best fitting in terms of χ^2 (11.52) and RMSE (4.69), it had lower R^2 value (0.552) compared with the Langmuir one (R^2 = 0.826, χ^2 = 12.40, RMSE = 5.97), while all the remaining models behaved unsatisfactorily. Therefore, interpretation of physicochemical mechanism responsible for Hg biosorption onto *C. vulgaris* biomass should be based on a combination of assumptions of those three models.

In particular, the best-fitting Dubinin-Radushkevich model allowed estimating a mean sorption energy (E = 0.427 kJ/mol) well lower than the lowest energy threshold assumed for chemical ion exchange (8 kJ/mol) [14], which confirms the occurrence of a physical biosorption mechanism in agreement with what suggested by the kinetic study. This value is also lower than those reported for Pb(II) (0.717 kJ/mol) and Zn(II) (0.759 kJ/mol) [26] and corresponds to a Polanyi potential in the range 0.040-0.71 kJ/mol and a constant of sorption energy of 2.74 mol^2/kJ^2.

The exponential parameter of Freundlich model was higher than unit (n = 2.78), and the Langmuir equilibrium parameter (R_L) in the range 0.156-0.605 (Table 4), which confirms that Hg biosorption is a very intense, favorable physical process. In addition, the satisfactory applicability of both Langmuir and Freundlich models highlights a medium term between heterogeneous monolayer and finite number of identical and homogeneous sites, in agreement with previous observations [5]. The Langmuir equilibrium constant (K_L), which is related to sorbent affinity for sorbate, was very high (0.0594 L/mg) and comparable with that reported by the same authors for Pb^{2+} adsorption by the same microorganism (11.3 L/mmol, equivalent to 0.0545 L/mg). Taking into account that at pH 5.0 Hg is partly present also as $Hg(OH)^+$, this result confirms the high affinity of such a biosorbent for Hg. On the other hand, less affinity was observed by the same authors for Zn^{2+} (K_L = 1.60 L/mmol, equivalent to 0.0245 L/mg) and mainly for Ni^{2+} (K_L = 0.0148 L/mg), which suggests that an increase in the distance from the nucleus makes the electrons less strongly attracted by it and then more available for adsorption.

4 Conclusions

Kinetics and equilibrium isotherms of mercury biosorption by dry *C. vulgaris* biomass were investigated in this work at variable initial metal concentration. The best kinetic and isotherm models to describe Hg removal were the pseudo first-order and Dubinin-Radushkevich ones, respectively. FT-IR spectroscopy suggested that Hg adsorption is favored under mildly acidic conditions and is likely to occur via physisorption. These results confirm that *C. vulgaris* biomass could be employed as cheap and efficient biosorbent to treat Hg-containing wastewater.

Acknowledgements The authors thanks prof. Elisabetta Finocchio for helpful discussion and interpretation of FT-IR data and acknowledge the financial support of the Italian Ministry of Education, University and Research to the Scientific Research Program of Relevant National Interest 2010-2011 (PRIN) “Emerging contaminants in air, soil, and water: from source to the marine environment” (grant number 2010WLNFY2_003).

Conflict of Interest The authors declare that they have no conflict of interest.

References

1. Krishnamoorthi CR, Vishwanathan P. Toxic metal in the Indian environment. New Delhi: Tata McGraw Hill Publishing Co. Ltd.; 1991.
2. Matheichal JT, Yu Q, Feltham J. Cu (II) binding by *E. radiata* biomaterial. Environ Technol 1997;18:25-34.
3. Ayangbenro AS, Babalola OO. A new strategy for heavy metal polluted environments: a review of microbial biosorbents. Int J Environ Res Public Health 2017;14(1):94. DOI: 10.3390/ijerph14010094.
4. Inthorn D, Sidtitoon N, Silapanuntakul S, Incharoensakdi A. Sorption of mercury, cadmium and lead by microalgae. Science Asia 2002;28:253-261.

5. Ferreira LS, Rodrigues MS, Carvalho JCM, et al. Adsorption of Ni^{2+}, Zn^{2+} and Pb^{2+} onto dry biomass of *Arthrospira (Spirulina) platensis* and *Chlorella vulgaris*. I. Single metal systems. Chem Eng J 2011;173:326–333.
6. Rodrigues MS, Ferreira LS, Carvalho JCM, et al. Metal biosorption onto dry biomass of *Arthrospira (Spirulina) platensis* and *Chlorella vulgaris*: multi-metal systems. J Hazard Mater 2012;217-218:246-255.
7. Finocchio E, Lodi A, Solisio C, et al. Chromium (VI) removal by methylated biomass of *Spirulina platensis*. Chem Eng J 2010;156:264–269.
8. Lodi A, Finocchio E, Converti A, et al. Removal of bivalent and trivalent ions by *Spirulina platensis* biomass: batch experiments and biosorbent characterisation. Int J Environ Technol Manag 2010;12:202–213.
9. Qiu H, Lv L, Pan B-C, et al. Critical review in adsorption kinetic models. J Zhejiang Univ Sci A 2009;10:716-724.
10. Samarghandi MR, Hadi M, Mohayedi S, et al. Two-parameter isotherms of methyl orange sorption by pinecone derived activated carbon. J Environ Health Sci Eng 2009;6:285-294
11. Sampranpiboon P, Charnkeitkong P, Feng X. Equilibrium isotherm models for adsorption of Zinc (II) ion from aqueous solution on pulp waste. WSEAS T Environ Dev 2014;10:35-47.
12. Bischoff HW, Bold HC. Phycological studies IV. Some soil algae from enchanted rock and related algal species, Austin, TX, USA: Univ. Austin University; 1963 (Publ. n. 6318).
13. Deng S, Ting YP. Fungal biomass with grafted poly (acrylic acid) for enhancement of Cu (II) and Cd (II) biosorption. Langmuir 2005;21:5940-5948.
14. Youssef AM, El-Khouly S, El-Nabarawy TH. Removal of Pb(II) and Cd(II) from aqueous solution using activated carbons from pecan shells. Carbon Lett 2008;9:8–13.
15. Herrero R, Lodeiro P, Rey-Castro C, et al. Removal of inorganic mercury from aqueous solutions by biomass of the marine macroalga *Cystoseira baccata*. Water Res 2005;29:3199-3210.
16. Vázquez G, González-Álvarez J, Freire S, et al. Removal of cadmium and mercury ions from aqueous solution by sorption on treated *Pinus pinaster* bark: kinetics and isotherms. Bioresour Technol 2002;82:247-251.
17. Zabihi M, Ahmadpour A, Asl AH. Removal of mercury from water by carbonaceous sorbents derived from walnut shell. J Hazard Mater 2009;167:230-236.
18. Daneshvar E, Sohrabi MS, Kousha M, et al. Shrimp shell as an efficient bioadsorbent for Acid Blue 25 dye removal from aqueous solution. J Taiwan Inst Chem Eng 2014;45:2926–2934.
19. Crini G, Badot P-M. Application of chitosan, a natural aminopolysaccharide, for dye removal from aqueous solutions by adsorption processes using batch studies: A review of recent literature. Prog Polym Sci 2008;33:399-447.
20. Khataee AR, Dehghan G, Ebadi A, et al. Biological treatment of a dye solution by macroalgae *Chara* sp.: effect of operational parameters, intermediates identification and artificial neural network modeling. Bioresour Technol 2010;101:2252-2258.
21. Gupta VK, Rastogi A. Biosorption of hexavalent chromium by raw and acid-treated green alga *Oedogonium hatei* from aqueous solutions. J Hazard Mater 2009;163:396-402.
22. Renault F, Morin-Crini N, Gimbert F, et al. Cationized starch-based material as a new ion-exchanger adsorbent for the removal of C.I. Acid Blue 25 from aqueous solutions. Bioresour Technol 2008;99:7573–7586.
23. Nirmal Kumar JI, Oommen C. Removal of heavy metals by biosorption using freshwater alga *Spirogyra hyalina*. J Environ Biol 2012;33:27-31.
24. Tüzün İ, Bayramoğlu G, Yalçın E, et al. Equilibrium and kinetic studies on biosorption of Hg(II), Cd(II) and Pb(II) ions onto microalgae *Chlamydomonas reinhardtii*. J Environ Manage 2005;77:85–92.
25. Zaib M, Athar M, Saeed A, et al. Equilibrium, kinetic and thermodynamic biosorption studies of Hg(II) on red algal biomass of *Porphyridium cruentum*. Green Chem Lett Rev 2016;9(4):179-189.
26. Yahaya LE, Akinlabi AK. Adsorptive removal of lead and zinc ions from aqueous solution using thiolated tea (*Camellia sinensis*) seed shell. Iranica Journal of Energy & Environment 2015;6:181-187.

Captions of Figures

Figure 1. FT-IR spectra of dry *Chlorella vulgaris* biomass before Hg adsorption a), and after Hg adsorption at pH 5.0 b) and pH 2.0 c).

Figure 2. Time behavior of A) the Hg biosorption capacity (q) of dry *Chlorella vulgaris* biomass and B) the ratio of Hg concentration to that at the beginning of runs (C/C_0). Hg concentration (mg/L): 11.0 (■), 17.0 (▲), 23.0 (●), 27.0 (○), 39.2 (△), 48.0 (□), 77.9 (◆), 90.6 (×). Temperature = 20°C, biomass concentration = 2.0 g/L.

Figure 3. Fitting of the pseudo-first order model to the experimental data of Hg biosorption capacity (q) of dry *Chlorella vulgaris* biomass at different metal concentrations (mg/L): 11.0 (■), 17.0 (▲), 23.0 (●), 27.0 (○), 39.2 (△), 48.0 (□), 77.9 (◆), 90.6 (×). Temperature = 20°C, biomass concentration = 2.0 g/L, q_e = biosorption capacity at equilibrium.

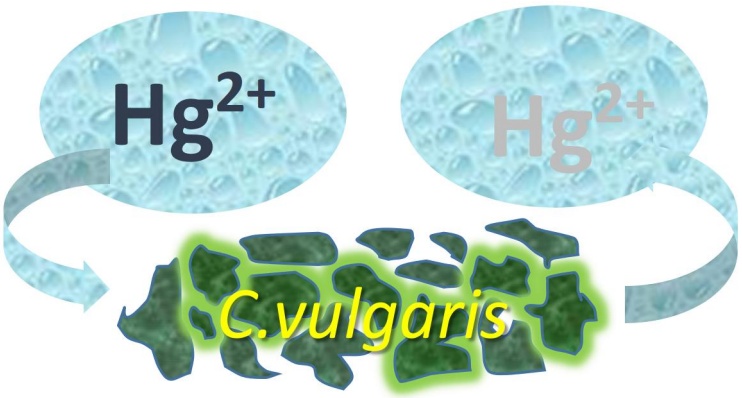

Graphical abstract

Adsorption of inorganic mercury from aqueous solutions onto dry biomass of *Chlorella vulgaris*: kinetic and isotherm studies

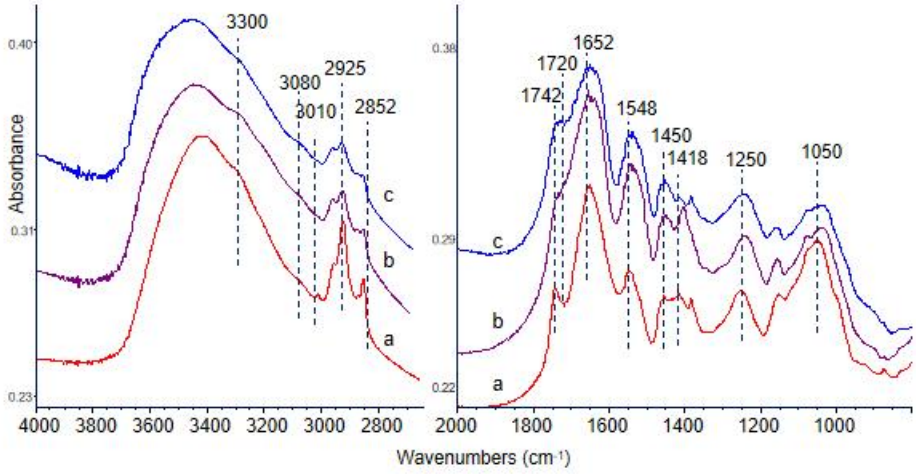
3300
3080
3010
2925
2852
1652
1720
1742
1548
1450
1418
1250
1050
Absorbance
Wavenumbers (cm-1)
a
b
c

Fig. 1

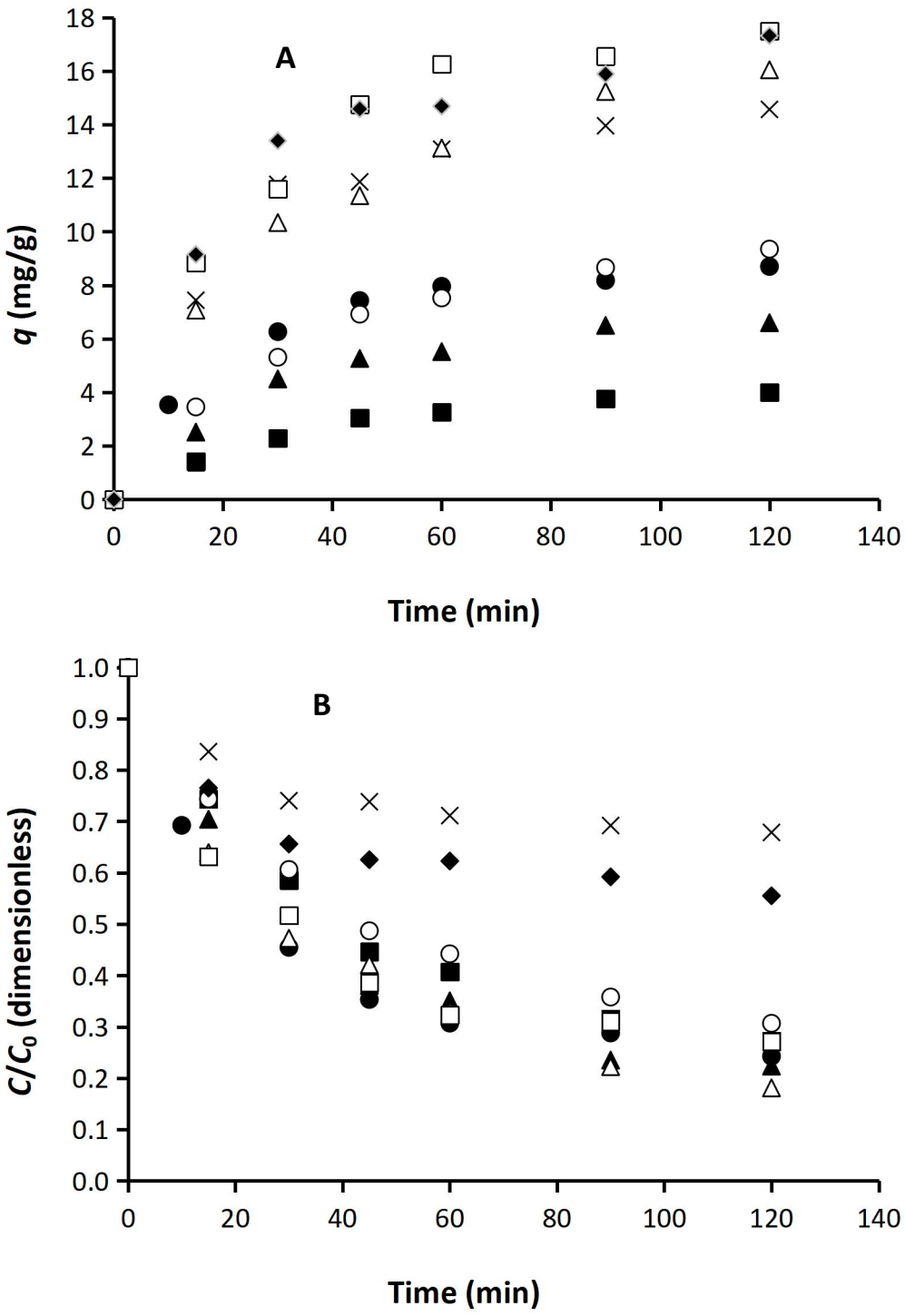

Fig. 2

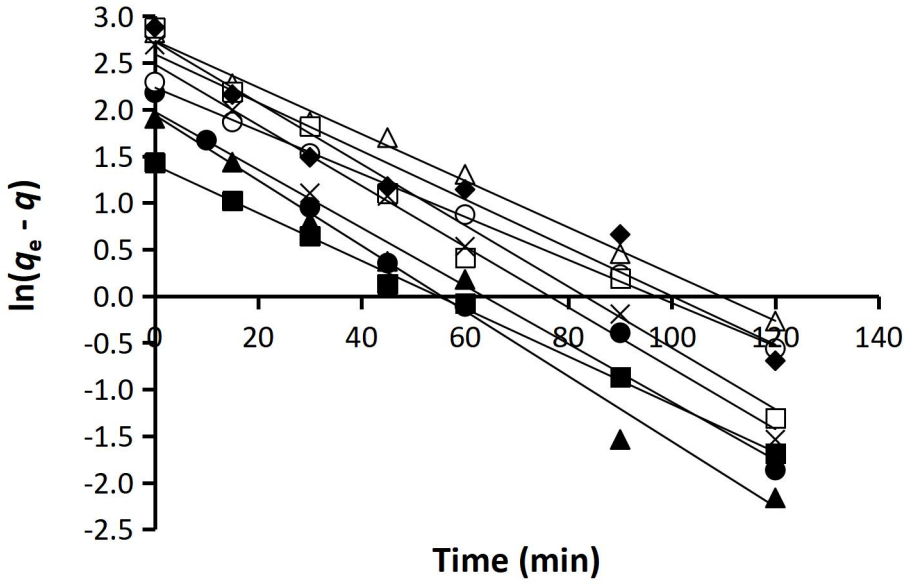
3.0
2.5
2.0
1.5
1.0
0.5
0.0
-0.5
-1.0
-1.5
-2.0
-2.5
0
20
40
60
80
100
120
140
ln(q_e - q)
Time (min)

Fig. 3

Table 1. Preliminary tests of Hg adsorption by dry biomass of *Chlorella vulgaris*. Biomass concentration = 2.0 g/L, temperature = 20°C.

C_0 (mg/L)	pH	C_e (mg/L)	q_e (mg/g)
25.0	2.0	12.1	6.45
43.7	2.0	22.0	10.8
23.0	5.0	9.3	8.86
39.2	5.0	5.6	16.8

Table 2. Main IR bands of *Chlorella vulgaris* biomass and their assignation [5].

Wavenumber (cm^{-1})	Assignation
3300 broad	NH stretching modes (amine and amide groups)
3080 weak	
3010 weak	=C-H stretching mode of unsaturated alkyl chains (lipid fraction)
2955-2871	Asymmetric CH stretching modes ($-CH_3$ and $-CH_2-$ groups)
2925-2852	Symmetric CH stretching modes ($-CH_3$ and $-CH_2-$ groups)
1742	C=O stretching mode (ester functional group of triglycerides and phospholipids fraction)
1650, 1548	Amide I and amide II vibrational modes (protein fraction)
1620 shoulder	Asymmetric stretching of the COO- group
1450	CH deformation modes
1416	Symmetric stretching of the COO- group
1250	C-O stretching mode of the ester/carboxylate groups
1050, broad, complex	CC/CO stretching modes (carbohydrate fraction)

Table 3. Kinetic parameters of Hg biosorption by dry biomass of *Chlorella vulgaris* estimated by different linearized adsorption models at different initial Hg concentrations. pH = 5.0; temperature = 20°C; biosorbent dosage = 2.0 g/L.

	Pseudo-first order			Pseudo-second order			Intraparticle diffusion			Simplified Elovich			Elovich			
C_0 (mg/L)	q_e (mg/g)	k_1 (min^{-1})	R^2	q_e (mg/g)	k_2 (g g^{-1} min^{-1})	R^2	C (mg/g)	k_{id} (mg g^{-1} $min^{-0.5}$)	R^2	a (mg g^{-1} min^{-1})	b (g/mg)	R^2	a (mg g^{-1} min^{-1})	b (g/mg)	t_0 (min)	R^2
11.0	4.19	0.026	0.997	5.38	4.72	0.995	0.29	0.36	0.940	0.27	0.79	0.988	0.18	0.65	8.8	0.978
17.0	6.72	0.035	0.982	8.41	3.99	0.990	1.09	0.55	0.893	0.56	0.51	0.966	0.41	0.45	5.5	0.952
23.0	8.86	0.031	0.969	9.90	6.03	0.998	2.44	0.63	0.866	1.31	0.48	0.965	1.06	0.45	2.1	0.957
27.0	9.92	0.023	0.996	12.35	2.12	0.999	0.79	0.82	0.959	0.64	0.35	0.995	0.43	0.29	8.1	0.989
39.2	16.81	0.025	0.994	19.92	1.70	0.996	2.88	1.26	0.971	1.46	0.23	0.995	1.09	0.20	4.5	0.992
48.0	17.76	0.033	0.970	20.41	2.54	0.995	5.31	1.21	0.878	2.40	0.23	0.949	2.00	0.22	2.3	0.944
77.9	17.82	0.026	0.990	19.19	3.33	0.996	6.76	1.00	0.870	3.85	0.28	0.940	3.47	0.27	1.1	0.937
90.6	14.78	0.033	0.976	16.50	3.79	0.997	5.50	0.90	0.837	2.83	0.31	0.921	2.51	0.30	1.3	0.916

Table 4. Application of different linearized adsorption isotherm models to Hg biosorption onto dry biomass of *Chlorella vulgaris* carried out at different initial Hg concentrations (11.0-90.6 mg/L). pH = 5.0; temperature = 20°C; biosorbent dosage = 2.0 g/L.

Model	Parameter	Unit	Value	χ^2	RMSE	R^2
Langmuir	q_0	(mg/g)	32.57			
	K_L	(L/mg)	0.0594	12.40	5.97	0.826
	R_L	(dimensionless)	0.156-0.605			
Freundlich	K_F	($mg^{1-1/n}$ $L^{1/n}$ g^{-1})	4.69	11.52	4.69	0.552
	n_F	(dimensionless)	2.78			
Temkin	K_T	(mg/L)	2.80	32.29	11.30	0.540
	b_T	(kJ/mol)	688.8			
Dubinin/Radushkevich	q_{DR}	(mg/g)	16.6			
	β	(mol^2/kJ^2)	2.74			
	ε	(kJ/mol)	0.040-0.71	3.47	2.76	0.870
	E	(kJ/mol)	0.427			
Harkins-Jura	$??_{HJ}$	(—)	40.16	NV	NV	0.415
	B_{HJ}	(—)	1.602			
Halsey	K_{Ha}	(—)	13.13	408.2	127.0	0.647
	n_{Ha}	(—)	1.99			
Jovanovic	q_0	(mg/g)	17.821	-14,705	5,189	0.074
	K_J	(L/mg)	0.1067			
Redlich-Peterson	K_{RP}	(L/g)	4.75			
	a_{RP}	(L^{γ}/mg^{γ})	0.523	56.07	7.85	0.764
	γ	(dimensionless)	0.780			

NV = not valid, because of too high values.